Hindawi
Wireless Communications and Mobile Computing
Volume 2020, Article ID 8857271, 9 pages
https://doi.org/10.1155/2020/8857271

Research Article

Image Dehazing Method of Transmission Line for Unmanned Aerial Vehicle Inspection Based on Densely Connection Pyramid Network

Jun Liu,[1,2] Rong Jia,[1] Wei Li,[1] Fuqi Ma,[3] and Xiaoyang Wang[4]

[1]*Xi'an University of Technology, 710048 Shaanxi Province, China*
[2]*State Grid Shaanxi Maintenance Company, 710065 Shaanxi Province, China*
[3]*School of Electrical Engineering and Automation, Wuhan University, Wuhan, China*
[4]*Guangzhou Power Supply Company, 210000 Guangzhou, Wuhan, China*

Correspondence should be addressed to Fuqi Ma; 18392647176@163.com

Received 14 July 2020; Revised 26 August 2020; Accepted 21 September 2020; Published 8 October 2020

Academic Editor: Panagiotis Sarigiannidis

The quality of the camera image directly determines the accuracy of the defect identification of the transmission line equipment. However, complex external factors such as haze can seriously affect the image quality of the aircraft. The traditional image dehazing methods are difficult to meet the needs of enhanced image inspection in complex environments. In this paper, the image enhancement technology in haze environment is studied, and an image dehazing method of transmission line based on densely connection pyramid network is proposed. The method uses an improved pyramid network for transmittance map calculation and uses an improved U-net network for atmospheric light value calculation. Then, the transmittance map, atmospheric light value, and dehazed image are jointly optimized to obtain image dehazing model. The method proposed in this paper can improve image brightness and contrast, increase image detail information, and can generate more realistic deblur images than traditional methods.

1. Introduction

In recent years, with the breakthrough of key transmission technologies such as intelligent autonomous operations and maintenance systems, UAV inspection [1–7] has been rapidly promoted and applied. For the patrol pictures, videos and other data generated during the patrol operation of the transmission line UAV, pattern recognition and computer vision technology [8–12] can be used to complete the discrimination work with the help of computers. This technology uses the deep learning network [13–18] to train and learn the fault samples of transmission line equipment, to obtain amature power vision target detection model, and automatically realize the target detection and fault location of the machine patrol image. The recognition accuracy and positioning accuracy of the target detection algorithm are positively correlated with the quality of the machine patrol image. The higher the image quality, the more effective the detection algorithm. However, drone inspections are mostly carried out in the wild, and their complex weather conditions play a crucial role in the quality of the photos taken. Due to environmental pollution, in recent years, a large range of haze weather has occurred in China, and the visibility of the field of vision has declined sharply.

Particulate matter in the atmosphere will seriously scatter the light coming into the camera, causing the brightness and contrast of transmission line pictures taken during drone patrols to decrease. The background image information is blurred, which ultimately leads to a serious degradation of image quality and the accuracy of image target detection. Therefore, it is urgent to study the image enhancement technology which is more suitable for the smog environment.

Image dehazing has always been a hot issue in the field of image enhancement. The research on image dehazing method at home and abroad is mainly divided into two categories: nonphysical methods based on image enhancement

and restoration methods based on imaging models [19–23]. The method of image enhancement is mainly to use the traditional image enhancement technology to directly filter the low-quality foggy image to remove the influence of noise in the image and restore the image clarity. The typical image dehazing method based on image enhancement includes histogram equalization [24–28], wavelet transform method, and Retinex algorithm [29–31]. The method based on image physical repair is mainly to study the degradation model of foggy image and inversely solve the optical imaging model to obtain the dehazing image. This method can retain the detailed information of the image and improve the authenticity of the image. It is the mainstream direction of the current research on dehazing algorithms, and its representative method is based on the partial differential equation dehazing method [32], defog method based on depth of field [33, 34], defog method based on a priori theory, and defog method based on deep learning [35–37]. In recent years, CNN networks have achieved great success in the fields of image segmentation, target detection, object classification, etc. Affected by this, more and more scholars have begun to introduce CNN networks into image dehazing algorithms. Literature [38–41] obtained the transmittance map of foggy images by establishing a shallow neural network and then used the image degradation model to achieve image dehazing. Literature [42, 43] combines convolutional neural networks and guided filters to achieve the restoration of foggy images. Image dehazing method based on convolutional neural network achieves good dehazing results in some specific scenarios, but the network depth is insufficient, and the network architecture has defects that lead to unsatisfactory effects on scenes with high fog density.

Through the study of the existing image dehazing method, it is found that the traditional image dehazing method relies heavily on prior knowledge [44]. The model is seriously simplified, and the detail information of the dehazing image is insufficiently restored. The image enhancement method does not consider the physical imaging model, but only improves the visual effect of the image by changing the contrast and gray value of the image; image restoration is based on the imaging physical model, using dark channel prior theory [45] to repair the haze image. Compared with image enhancement, this method has better dehazing effect, but there are some simplifications to the image generation model during the implementation process, and there is still a certain difference between the restored image and the real image. In view of the shortcomings of the traditional image dehazing method, this paper proposes the image dehazing method of transmission line machine patrol image based on densely connected pyramid network. It directly embeds the atmospheric degradation model into the deep learning framework and uses physical principles to restore the image fog. The fog image obtained by this method is closer to the real image in visual effect.

2. Single Image Defog Model

2.1. Haze Image Optical Attenuation Model. In the field of image processing, the model [46] shown in Equation (1) is often used to describe the image formation process in fog and haze.

$$I(z) = J(z)t(z) + A(1 - t(z)). \tag{1}$$

Among them, I represents the real image taken by the camera in the case of fog and haze; J represents the clear picture taken in the case of clear weather. A is the ambient light intensity, which is usually assumed to be constant in the local area of the image; t is the transmittance, which is used to describe the proportion of light that enters the camera lens through the haze; z represents the position of the pixel in the image. Transmittance is a factor related to distance, which represents the proportion of light transmitted by the target object through the atmosphere and reaching the camera lens. When the atmospheric light value A in the local area of the image is constant, the transmittance can usually be expressed as Equation (2).

$$t(z) = e^{-\beta d(z)}. \tag{2}$$

It can be seen from Equation (1) that the image taken in fog and haze is the superposition of the light passing through the fog and the atmospheric light scattered by the fog and haze in a clear background image. The process of image dehazing is to find the global atmospheric light value A and transmittance t from the foggy image I, inversely calculate Equation (1), and finally obtain the clear image J.

2.2. Model Architecture of Densely Connected Pyramid Dehazing Network. This paper proposes a new deep learning-based transmission line machine patrol image dehazing network, called dense connection pyramid dehazing network (DCPDN). The network uses the method of end-to-end learning to achieve the purpose of image dehazing. The essence of the DCPDN network is to use the physical method of image restoration to solve the problem of image degradation. The end-to-end image dehazing repair is achieved by embedding the atmospheric degradation model Equation (1) into the deep learning network. In the dehazing network, the deep fusion between the transmittance map estimation module, the atmospheric light value estimation module, and the dehazing image is realized, and the information exchange and restriction between the various modules are achieved to achieve the purpose of common optimization.

The architecture of the DCPDN network proposed in this paper is shown in Figure 1. The network is composed of four parts: (1) a transmission diagram estimation module with densely connected pyramids, (2) atmospheric light value estimation module, (3) dehazing module based on image degradation equation, and (4) joint discriminator module. The four modules are introduced in detail below:

2.2.1. Pyramid Densely Connected Transmission Graph Estimation Network. Inspired by the previous method using multilevel features to estimate the transmittance map [47–51], this paper also attempts to use the multilevel features of the image to estimate the transmittance map, as shown

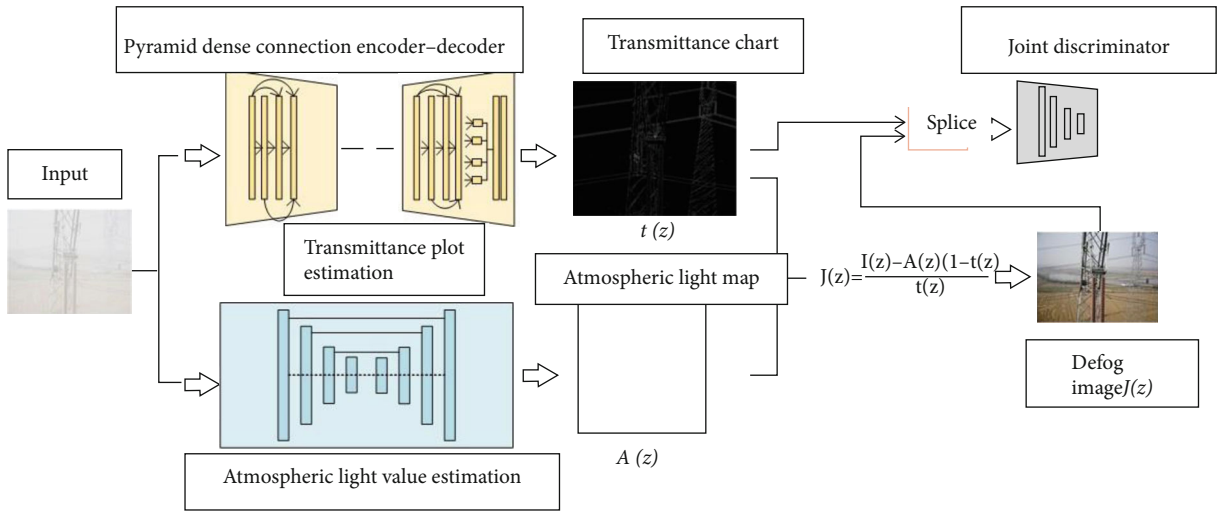

Figure 1: Densely connected pyramid dehazing network.

in Figure 2. A densely connected encoding-decoding structure is proposed. The encoder-decoder uses dense blocks as the basic structural unit, and dense connections are made between layers within the dense blocks. Dense blocks can not only use CNN network to extract multilevel features of the image, but also ensure better convergence of the entire encoding-decoding network. In addition, the encoder-decoder also uses a multilayer pyramid pooling module, which uses the global transmission information of the image to estimate the transmittance map, avoiding the problem that the network pays too much attention to local details and ignores the global information.

In the encoder, it is a first traditional convolution block and then four dense blocks. The output of the encoder is 1/32 of the original input image. Corresponding to the encoder is the decoder, whose structure is completely symmetrical with the encoder and contains four dense blocks and one convolution block. The output of the decoder and the original image have the same size, and the corresponding modules of the two are directly connected. Although the proposed densely connected encoding-decoding structure combines different features within the network, the transmittance graph output only through the encoder-decoder still lacks global structural information with different scale features. This is because the features extracted from the images of different scales are not directly used to generate the feature rate map, so after the codec, the network has added a multilevel pyramid pooling module to use the feature information obtained by each layer of the feature pyramid. The final transmittance map is estimated. The pyramid pooling module designed in this paper contains four levels of pooling operations, and the output size is 1/4, 1/8, 1/16, and 1/32 of the original image size. Then, all the four sizes of transmittance maps are upsampled to the original image size, and the original images are connected, respectively, and finally, the fined transmittance map is obtained.

2.2.2. Atmospheric Light Value Estimation Network. The calculation of atmospheric light values in the traditional image dehazing method is based on empirical formulas. The atmospheric light map used for dehazing is also rough and not precise, so it is difficult to obtain satisfactory dehazing images. This network proposes an improved U-net network when solving atmospheric light values, as shown in Figure 3. The entire network includes two parts: upsampling and downsampling. The upsampling process is to capture the context information of the image, and the downsampling process is to obtain the local precise information of the image. In the downsampling process, every two 3×3 convolutional layers will be followed by a 2×2 pooling layer. ReLU is used as the activation function after each convolutional layer. The upsampling process is symmetrical with the downsampling process. Each 2×2 pooling layer is followed by two 3×3 convolutional layers. The high-pixel atmospheric light feature maps extracted during the downsampling process are directly transmitted to the corresponding upsampling process to guide the generation of new feature maps and retain some of the important feature information obtained during the previous downsampling process to the greatest extent. The final output of the network is a refined atmospheric light map. The value of each pixel in the picture is as close as possible to the atmospheric light value in the case of real haze.

2.2.3. Dehazing Module Based on Image Degradation Equation. In order to realize image dehazing using physical imaging principles, this network directly embeds the image degradation model into the dehaze network. As shown in the dehazing module in Figure 1, accurate transmittance map and atmospheric light map can be obtained from the first two modules, and the dehazing image can be easily obtained by using the image degradation model.

2.2.4. Joint Optimization Discriminant Network. In order to establish the relationship between transmittance map, atmospheric light map, and dehazing image, this paper builds a joint optimization discriminant network based on GAN network [51]. The discrimination network uses the high

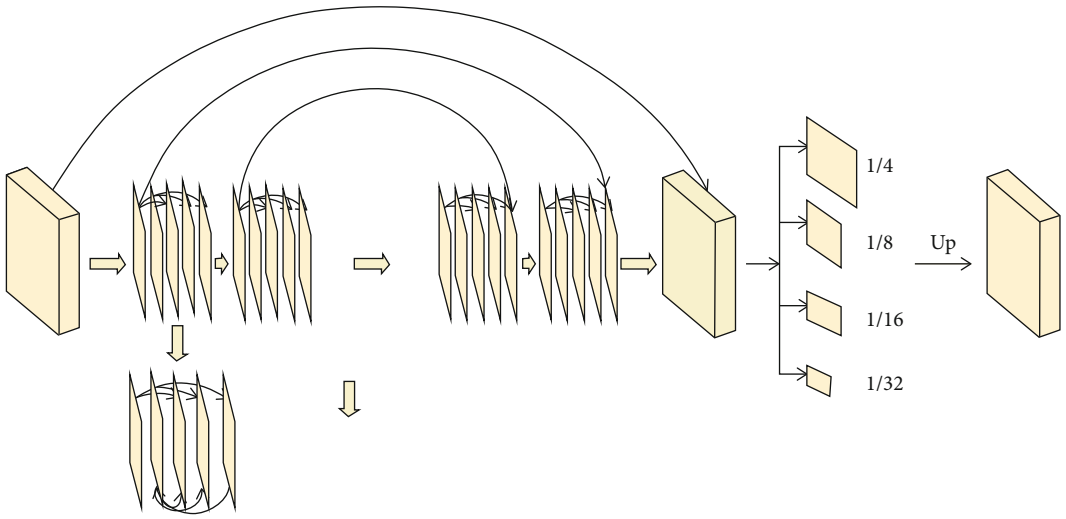

Figure 2: Densely connected encoding-decoding structure.

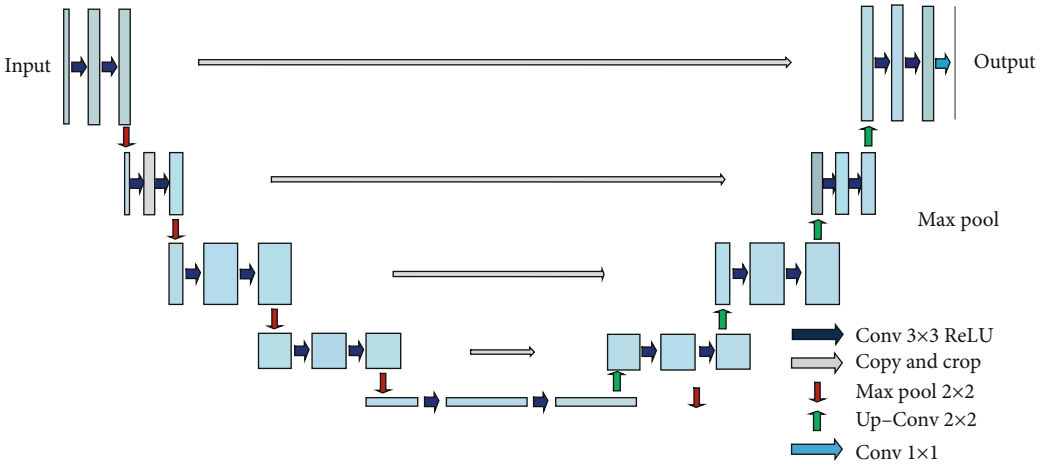

Figure 3: Atmospheric light value estimation network.

correlation between the three to optimize the generated transmittance map, atmospheric light map, and dehazing image and finally obtain a clear and true dehazing image. Let$G_t$and G_d denote the generation networks of clear images and transmittance maps respectively. As shown in Equation (3), the first part and the second part of the formula are the games between the generator and the discriminator. Continuously optimize the generation and discrimination network and finally be able to generate the transmittance map and dehazing image as realistic as possible. The third part of the formula is to compare the actual clear image with the defogged image to further optimize the dehazing image.

$$\begin{aligned}\min_{G_t,G_d}\max_{D_{\text{joint}}} & E_{I\sim p_{\text{data}(I)}}\left[\log\left(1-D_{\text{joint}}(G_t(I))\right)\right]\\ & + E_{I\sim p_{\text{data}(I)}}\left[\log\left(1-D_{\text{joint}}(G_d(I))\right)\right]\\ & + E_{t,J\sim p_{\text{data}(t,J)}}\left[\log D_{\text{joint}}(G_t(t,J))\right].\end{aligned} \tag{3}$$

2.3. Defog Network Loss Function

2.3.1. Edge Protection Loss Function. For the training of deep learning networks, the simplest loss function is the L2 loss function, but after many experiments, it is found that only the L2 loss function is used for network training, and the output image is often blurred. Through in-depth analysis of the image, it is found that the value of the edge pixel point of the target object has a discontinuity. It can be characterized by calculating the gradient of the pixel value. The edge and contour features of the target object can be captured in the first few layers of the CNN structure, so the first few layers of the convolutional neural network can be used as the edge detector for target feature extraction. So the first few layers of the convolutional neural network can be used as the edge detector for target feature extraction. Based on the above analysis, this paper proposes an edge protection loss function, which adds a two-way gradient loss and feature edge loss on the basis of the L2 loss function. The function expression is shown in Equation (4).

$$L^E = \lambda_{E,l_2}L_{E,l_2} + \lambda_{E,g}L_{E,g} + \lambda_{E,f}L_{E,f}. \tag{4}$$

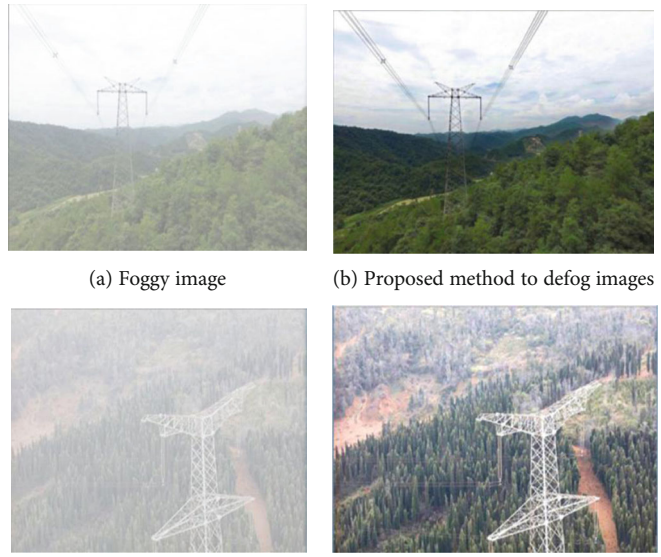

(a) Foggy image (b) Proposed method to defog images

(c) Foggy image (d) Proposed method to defog images

Figure 4: Image dehazing result graph.

L^E is the retention losses for the entire edge of the target object, L_{E,l_2} is the loss for L2, $L_{E,g}$ is for the horizontal and vertical gradient loss, and$L_{E,f}$ is a characteristic loss. The specific calculation formula of loss is shown in Equation (5).

$$L_{E,g} = \sum_{w,h} \left\| \left(H_x(G_t(I))\right)_{w,h} - \left(H_x(t)\right)_{w,h} \right\|_2 + \left\| \left(H_y(G_t(I))\right)_{w,h} - \left(H_y(t)\right)_{w,h} \right\|_2. \tag{5}$$

H_x and H_y calculate the image pixel gradient along the horizontal and vertical, respectively, and $w \times h$ represents the width and height of the output feature map. Feature loss definition is shown in Equation (6).

$$L_{E,f} = \sum_{c_1,w_1,h_1} \left\| \left(V_1(G_t(I))\right)_{c_1,w_1,h_1} - \left(V_1(t)\right)_{c_1,w_1,h_1} \right\|_2 + \sum_{c_2,w_2,h_2} \left\| \left(V_2(G_t(I))\right)_{c_2,w_2,h_2} - \left(V_2(t)\right)_{c_2,w_2,h_2} \right\|_2. \tag{6}$$

V_i is on behalf of the CNN structure, c_i, w_i, h_i, V_i are the dimension of the corresponding low-level feature.λ_{E,l_2}, $\lambda_{E,g}$, and$\lambda_{E,f}$ are the weight of the balance loss function.

2.3.2. Overall Loss Function. For the entire network training, in addition to the edge protection loss function, the loss function of the atmospheric light map, the loss function of the dehazing module, and the loss function of the joint optimization discriminator are also required. The overall loss function can be expressed as Equation (7).

$$L = L^t + L^a + L^d + \lambda_j L^j. \tag{7}$$

L^t consists of edge retention loss L^Ex, and L^a is the loss function of the atmospheric light calculation module that is composed of the traditional L2 loss L^d, which denotes defog loss, which also consists of L2 loss only.L^j is for the joint discriminator loss, andL^j is defined as Equation (8).

$$L^j = -\log\left(D_{\text{joint}}(G_t(I)) - \log\left(D_{\text{joint}}(G_d(I)), \right.\right. \tag{8}$$

where j is a constant.

3. Model Training

3.1. Composition of the Dataset. In order to train the dense connection pyramid dehazing network (DCPDN), this paper constructs a training set containing 8000 images through simulation. The training set contains a total of four data types, namely, foggy images, clear images, transmittance maps, and atmospheric light maps. In the process of obtaining the training set through simulation, we randomly sample as the atmospheric light value in the range of 0.5–1, And construct of the corresponding atmospheric light map, we randomly select the data as the scattering coefficient in the range of 0.4–1.6 and generate the corresponding transmittance map. We randomly selected 2000 transmission line images captured by drone patrol under clear weather and synthesized them according to the foggy image model Equation (1), obtaining a total of 8000 simulation images. Then, the dataset is divided into training set, validation set, and test set according to 7 : 2 : 1. In order to ensure that the trained dehazing network has good generalization performance, the training set in this paper does not contain any pictures in the verification test set.

3.2. Training Details of the Dehazing Network. In the model training process, we choose $\lambda_{E,l_2} = 1$, $\lambda_{E,g} = 0.5$, and $\lambda_{E,f} = 0.8$ in the transmission graph as parameters of the loss function, $\lambda_j = 0.25$. As a parameter of the loss function, the joint optimization discriminator is optimized. The entire network

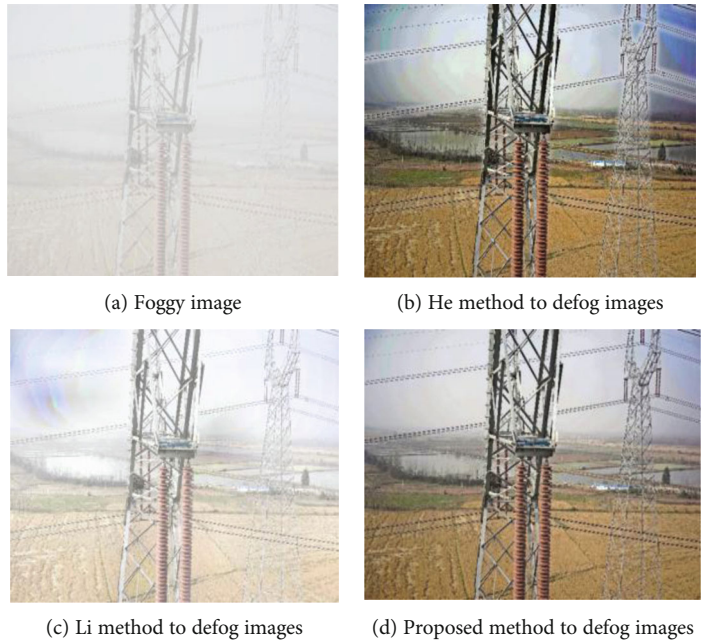

(a) Foggy image (b) He method to defog images

(c) Li method to defog images (d) Proposed method to defog images

Figure 5: Contrast of image dehazing result.

Table 1: PSNR and SSIM of dehazing image.

Method	PSNR	SSIM
He image dehazing method	18.9613	0.7753
Li image dehazing method	18.7452	0.8374
DCPDN image dehazing method	19.6954	0.8478

uses Gaussian random variables to initialize the weight parameters, and the Adam optimization algorithm is used to optimize the network. The initial learning rate of the generator and the joint discriminator is set to 2×10^{-3}. The learning rate is a key parameter that affects the model training.

The smaller the learning rate, the less likely to miss the local minimum, but the smaller the learning rate, the slower the model convergence. The number of samples in the training set of this network is not very large, so the full training set is selected for the batch size. Each iteration of the network can make full use of the feature information of the data in the entire training set and can accelerate the network's approach to the extreme point. In addition, the size of the image input from the network is uniformly adjusted to 512 $\times$ 512. In the end, the paper performed 40,000 iterations on the network and determined all the parameters of the network through cross-validation.

During the initial training of the model, we found that starting to train the entire network directly, the convergence speed of the network is very slow. The possible reason is that the gradient descent direction of different modules in the network in the initial training period is inconsistent, causing the convergence speed of the entire network to decrease. In order to solve this problem and accelerate training, this method introduces a staged learning strategy, which has been used in multimodel recognition [52] and feature learning [53] The algorithm is applied. We input the information in the training data to different modules in the network, and each module is trained separately without affecting each other, and we update the parameters independently. After each module completes the "initialization" of parameters, we associate different modules with each other to jointly optimize the entire network.

4. Analysis of Experimental Results

4.1. Defog Image Rendering Comparison. We randomly select a foggy image from the UAV inspection image sample library and use the DCPDN dehazing algorithm for dehazing. The results are shown in Figure 4.

Figures 4(a) and 4(c) are the original foggy images. Figures 4(b) and 4(d) are the images after DCPDN method. It can be seen from Figure 4 that the method in this paper can effectively remove the haze in the image and restore the image detail information.

We randomly select a foggy image from the UAV inspection image sample library and use the He dehazing algorithm [37], Li dehazing algorithm [38], and DCPDN dehazing algorithm for dehazing. The results are shown in Figure 5.

Figures 5(a)–5(d) are the original foggy image, the image after He dehazing method, the image after Li dehazing method, and the image after DCPDN method, respectively. It can be seen from Figure 5(b) that the image processed by the He image dehazing method is seriously distorted in the sky area, and it is not good for dehazing images containing large white areas. It can be clearly seen from Figure 5(c) that the image dehazing is not thorough enough. The main reason is that the CN method used in the Li method has fewer layers, and the fog feature extraction is insufficient, resulting in the presence of fog in the processed image. Figure 5(d) is the result obtained by adopting the new dehazing network

Table 2: Target detection results.

	Tower failure (AP)	Small-size fittings (AP)	Ground wire fault (AP)	Insulator failure (AP)	mAP
Foggy image	0.5746	0.4368	0.5128	0.5974	0.5304
He defog image	0.6417	0.4985	0.5847	0.6187	0.5859
Li defog image	0.6239	0.5018	0.6017	0.6245	0.5880
This article method	0.7828	0.5786	0.6451	0.7013	0.6770

proposed in this paper. From the visual effect, it is obviously superior to the first two methods, and the image detail information is restored while ensuring the image brightness and contrast.

4.2. Comparison of Dehazing Image Indicators. Peak signal-to-noise ratio (PSNR) and structural similarity (SSIM) are often used as the basis for image quality evaluation. The peak signal-to-noise ratio is defined by the ratio of the maximum signal power to the signal noise power, usually expressed in decibels. Structural similarity is to evaluate the image quality from the image brightness, contrast, and structural properties of the target object. We calculate the PSNR and SSIM values of Figure 5, and the results are shown in Table 1.

It can be seen from the comparison of the PSNR value and SSIM value in Table 1 that the DCPDN image dehazing method proposed in this paper is better than the image dehazing method of He and Li, and the PSNR value and SSIM value are higher. It shows that the image dehazing method proposed in this paper is good for image repair and can generate dehazing images with high similarity to clear images.

4.3. Target Detection Accuracy Comparison. In the field of target detection, two indicators, average precision (AP) and mean average precision (mAP), are usually used to evaluate the pros and cons of the target detection algorithm. The average accuracy is used to measure the recognition accuracy of a target detection algorithm for an object. The mean average accuracy is used to measure the recognition accuracy of an algorithm on all targets. Generally speaking, mAP is a simple average of multitarget detection AP.

From the test set, 100 randomly selected images of foggy transmission lines with pole tower failure, small-size fitting failure, ground conductor failure, and insulator failure were selected. The He image dehazing method, Li image dehazing method, and DCPDN image dehazing method were used for image dehazing, respectively. The Faster Rcnn target detection algorithm [54] was used to detect the equipment defect targets for foggy images, He dehazing images, Li dehazing images, and DCPDN dehazing images. We calculate the AP values of the four faults and the mAP values of each group of images separately. The results are shown in Table 2.

It can be seen from the results in Table 2 that the AP value and mAP value of the target detection algorithm after image dehazing have been improved, and the effect of the method proposed in this article is the most obvious, indicating that the preprocessing of image dehazing can improve the accuracy of target detection. The AP value of the target detection algorithm for tower failure, ground conductor failure, and insulator failure has been greatly improved. The AP value of small-size metal fittings has a small increase, which proves that the image dehazing process can improve the overall image quality, and the effect of recovering the edge information of large-size target objects is obvious.

5. Conclusion

This paper proposes an image dehazing method of transmission line machine patrol image based on densely connected pyramid network. It embeds the atmospheric degradation model directly into the deep learning framework and uses physical principles to restore the image. For the calculation of the transmittance graph, this paper proposes a new dense connection encoding-decoding structure with multilevel pooling modules and redesigns the edge retention loss function. This method introduces a joint discriminant optimizer based on GAN network in the network, which can jointly optimize the transmittance map and dehazing image with high correlation. Then use the sample set designed in this paper to train the network to obtain an image dehazing model suitable for the transmission line background. Experiments show that the dehazing image obtained by the method proposed in this paper is closer to the real image in visual effect. Using the dehazing algorithm proposed in this paper for image enhancement can improve the accuracy of the target detection algorithm.

Although the proposed method indeed promotes the quality of transmission line UAV inspection image, it is still not a real-time solution. Considering the actual problem that for the deep learning model proposed in this paper, the number of existing samples is still insufficient and future work can further increase the number of training set samples through data expansion method. In addition, the main work carried out in this paper is to enhance the image containing haze, but there are still some problems in the actual aircraft patrol image including raindrop image and motion blur. Thus, there is an important and meaningful need for work in the future to explore more comprehensive image enhancement method for unmanned aerial vehicle inspection in complex environment.

Abbreviations

CNN: Convolutional neural network
UAV: Unmanned aerial vehicle
DCPDN: Densely connection pyramid network
PSNR: Peak signal-to-noise ratio
SSIM: Structural similarity
AP: Average precision.

Data Availability

The authors do not share the data, due to the requirements of the foundations.

Conflicts of Interest

The authors declare that they have no competing interests.

Acknowledgments

The authors would like to thank the anonymous reviewers for their helpful insights and suggestions which have substantially improved the content and presentation of this paper. This work was supported by the National Natural Science Foundation of China (No. 51777142, No. 71371127, No. 91846301, No. 71790615, No. 51779206, and No. 71431006), the Key Project for Philosophy and Social Sciences Research of Shenzhen City (No. 135A004), Key Project of Natural Science Basic Research Plan in Shaanxi Province of China (Grant No. 2019ZDLGY18-03), and the Fundamental Research Funds for the Central Universities (Program No. 2722019PY052).

References

[1] A. Lytos, T. Lagkas, P. Sarigiannidis, M. Zervakis, and G. Livanos, "Towards smart farming: systems, frameworks and exploitation of multiple sources," *Computer Networks*, vol. 172, article 107147, 2020.

[2] F. J. Chen Miyun, *Exploration of the application of drones in the inspection of transmission lines*, Electrical Technology, 2019.

[3] C. Chen, C. Wang, T. Qiu, M. Atiquzzaman, and D. O. Wu, "Caching in vehicular named data networking: architecture, schemes and future directions," *IEEE Communications Surveys & Tutorials*, 2020.

[4] P. Radoglou-Grammatikis, P. Sarigiannidis, T. Lagkas, and I. Moscholios, "A compilation of uav applications for precision agriculture," *Computer Networks*, vol. 172, article 107148, 2020.

[5] C. Chen, J. Hu, T. Qiu, M. Atiquzzaman, and Z. Ren, "Cvcg: cooperative v2v-aided transmission scheme based on coalitional game for popular content distribution in vehicular ad-hoc networks," *IEEE Transactions on Mobile Computing*, vol. 18, no. 12, pp. 2811–2828, 2019.

[6] J. Hu, C. Chen, T. Qiu, and Q. Pei, "Regional-Centralized Content Dissemination for Ev2x Services in 5g Mmwave-Enabled IoV," *IEEE Internet of Things Journal*, vol. 7, no. 8, pp. 7234–7249, 2020.

[7] H. Chen, X. Wang, Z. Li, W. Chen, and Y. Cai, "Distributed sensing and cooperative estimation/detection of ubiquitous power internet of things," *Protection and Control of Modern Power Systems*, vol. 4, no. 1, 2019.

[8] S. Wan, Y. Xia, L. Qi, Y.-H. Yang, and M. Atiquzzaman, "Automated Colorization of a Grayscale Image with Seed Points Propagation," *IEEE Transactions on Multimedia*, vol. 22, no. 7, pp. 1756–1768, 2020.

[9] L. Yuling, *Computer vision technology and its application in power system automation*, China New Technology New Products, 2012.

[10] L. Li, T.-T. Goh, and D. Jin, "How textual quality of online reviews affect classification performance: a case of deep learning sentiment analysis," *Neural Computing and Applications*, vol. 32, no. 9, pp. 4387–4415, 2020.

[11] Y. Zhao, H. Li, S. Wan et al., "Knowledge-aided convolutional neural network for small organ segmentation," *IEEE Journal of Biomedical and Health Informatics*, vol. 23, no. 4, pp. 1363–1373, 2019.

[12] D. Jin, S. Shi, Y. Zhang, H. Abbas, and T.-T. Goh, "A complex event processing framework for an adaptive language learning system," *Future Generation Computer Systems*, vol. 92, pp. 857–867, 2019.

[13] Z. D. W. Shuai and X. Yong, "A survey of target detection based on deep convolutional networks," *Pattern Recognition and Artificial Intelligence*, vol. 31, no. 4, pp. 335–346, 2018.

[14] T.-T. Goh, Z. Xin, and D. Jin, "Habit formation in social media consumption: a case of political engagement," *Behaviour & Information Technology*, vol. 38, no. 3, pp. 273–288, 2019.

[15] S. Ding, S. Qu, Y. Xi, and S. Wan, "Stimulus-driven and concept-driven analysis for image caption generation," *Neurocomputing*, vol. 398, pp. 520–530, 2020.

[16] Z. Gao, H. Z. Xuan, H. Zhang, S. Wan, and K. K. R. Choo, "Adaptive fusion and category-level dictionary learning model for multiview human action recognition," *IEEE Internet of Things Journal*, vol. 6, no. 6, pp. 9280–9293, 2019.

[17] S. Wan and S. Goudos, "Faster R-CNN for multi-class fruit detection using a robotic vision system," *Computer Networks*, vol. 168, p. 107036, 2020.

[18] Z. Hu, T. He, Y. Zeng et al., "Fast image recognition of transmission tower based on big data," *Protection and Control of Modern Power Systems*, vol. 3, no. 1, article 15, 2018.

[19] Z. H. Chen Gong and T. Wang, "A new method for foggy image restoration based on physical model," *Journal of Image and Graphics*, vol. 13, no. 5, pp. 888–893, 2008.

[20] S. Ding, S. Qu, Y. Xi, and S. Wan, "A long video caption generation algorithm for big video data retrieval," *Future Generation Computer Systems*, vol. 93, pp. 583–595, 2019.

[21] C. Chen, T. Xiao, T. Qiu, N. Lv, and Q. Pei, "Smart-contract-based economical platooning in blockchain-enabled urban internet of vehicles," *IEEE Transactions on Industrial Informatics*, vol. 16, no. 6, pp. 4122–4133, 2020.

[22] C. Chen, X. Liu, T. Qiu, and A. K. Sangaiah, "A short-term traffic prediction model in the vehicular cyber–physical systems," *Future Generation Computer Systems*, vol. 105, pp. 894–903, 2020.

[23] Z. Gao, Y. Li, and S. Wan, "Exploring deep learning for view-based 3d model retrieval," *ACM Transactions on Multimedia Computing, Communications, and Applications*, vol. 16, no. 1, pp. 1–21, 2020.

[24] F. Russo, "An image enhancement technique combining sharpening and noise reduction," *IEEE Transactions on Instrumentation and Measurement*, vol. 51, no. 4, pp. 824–828, 2002.

[25] Z. Lv, B. Hu, and H. Lv, "Infrastructure monitoring and operation for smart cities based on iot system," *IEEE Transactions on Industrial Informatics*, vol. 16, no. 3, pp. 1957–1962, 2020.

[26] Z. Lv, W. Kong, X. Zhang, D. Jiang, H. Lv, and X. Lu, "Intelligent security planning for regional distributed energy internet," *IEEE Transactions on Industrial Informatics*, vol. 16, no. 5, pp. 3540–3547, 2020.

[27] Z. Lv, X. Li, H. Lv, and W. Xiu, "Bim big data storage in WebVRGIS," *IEEE Transactions on Industrial Informatics*, vol. 16, no. 4, pp. 2566–2573, 2020.

[28] J. Y. Kim, L. S. Kim, and S. H. Hwang, "An advanced contrast enhancement using partially overlapped sub-block histogram equalization," *IEEE Transactions on Circuits and Systems for Video Technology*, vol. 11, no. 4, pp. 475–484, 2001.

[29] Z.-u. Rahman, D. J. Jobson, and G. A. Woodell, "Retinex processing for automatic image enhancement," *Journal of Electronic Imaging*, vol. 13, no. 1, pp. 100–110, 2004.

[30] D. J. Jobson, Z. Rahman, and G. A. Woodell, "A multiscale retinex for bridging the gap between color images and the human observation of scenes," *IEEE Transactions on Image Processing*, vol. 6, no. 7, pp. 965–976, 1997.

[31] L. Meylan and S. Susstrunk, "High dynamic range image rendering with a retinex-based adaptive filter," *IEEE Transactionson Image Processing*, vol. 15, no. 9, pp. 2820–2830, 2006.

[32] Y. S. Zhai, X. M. Liu, and Y. Y. Tu, "Contrast enhancement algorithm for fog-degraded image based on fuzzy logic," *Journal of Computer Applications*, vol. 28, no. 3, pp. 662–664, 2008.

[33] J. P. Oakley and B. L. Satherley, "Improving image quality in poor visibility conditions using a physical model for contrast degradation," *IEEE Transactions on Image Processing*, vol. 7, no. 2, pp. 167–179, 1998.

[34] N. Hautiere, J. P. Tarel, and D. Aubert, "Towards fog-free in-vehicle vision systems through contrast restoration," in *2007 IEEE Conference on Computer Vision and Pattern Recognition*, pp. 1–8, Minneapolis, MN, USA, June 2007.

[35] S. Wan, X. Xu, T. Wang, and Z. Gu, "An intelligent video analysis method for abnormal event detection in intelligent transportation systems," *IEEE Transactions on Intelligent Transportation Systems*, pp. 1–9, 2020.

[36] R. Fattal, "Single image dehazing," *ACM Transactions on Graphics*, vol. 27, no. 3, p. 72, 2008.

[37] K. He, J. Sun, and X. Tang, "Single image haze removal using dark channel prior," in *2009 IEEE Conference on Computer Vision and Pattern Recognition*, pp. 1956–1963, Miami, FL, USA, June 2009.

[38] C. Li, J. Guo, F. Porikli, C. Guo, H. Fu, and X. Li, "Dr-Net: transmission steered single image dehazing network with weakly supervised refinement," in *2017 IEEE Conference on Computer Vision and Pattern Recognition (CVPR)*, pp. 1–8, Honolulu, HI, USA, 2017.

[39] H. Yang, J. Pan, Q. Yan, W. Sun, J. Ren, and Y. Tai, "Image dehazing using bilinear composition loss function," in *2017 IEEE Conference on Computer Vision and Pattern Recognition (CVPR)*, pp. 1–9, Honolulu, HI, USA, 2017.

[40] R. Liu, X. Fan, M. Hou, Z. Jiang, Z. Luo, and L. Zhang, "Learning aggregated transmission propagation networks for haze removal and beyond," *IEEE Transactions on Neural Networks*, vol. 30, no. 10, pp. 2973–2986, 2019.

[41] H. Zhang, V. A. Sindagi, and V. M. Patel, "Joint transmission map estimation and dehazing using deep networks," in *2017 IEEE Conference on Computer Vision and Pattern Recognition (CVPR)*, pp. 1–11, Honolulu, HI, USA, 2017.

[42] Y. Song, J. Li, X. Wang, and X. Chen, "Single image dehazing using ranking convolutional neural network," *IEEE Transactions on Multimedia*, vol. 20, no. 6, pp. 1548–1560, 2018.

[43] X. Zhao, K. Wang, Y. Li, and J. Li, "Deep fully convolutional regression networks for single image haze removal," in *2017 IEEE Visual Communications and Image Processing (VCIP)*, pp. 1–4, St. Petersburg, FL, USA, December 2017.

[44] X. Z. Dong Haoyuan, "Blind quantization noise estimation algorithm based on prior knowledge of images," *Computer Engineering*, vol. 36, no. 11, pp. 195–197, 2010.

[45] B. H. Yang Aiping, "Night image defogging algorithm based on retinex theory and dark channel prior," *Progress in Laser and Optoelectronics*, vol. 54, no. 4, pp. 141–147, 2017.

[46] S. G. Narasimhan and S. K. Nayar, "Chromatic framework for vision in bad weather," in *Proceedings IEEE Conference on Computer Vision and Pattern Recognition. CVPR 2000 (Cat. No.PR00662)*, vol. 1, pp. 598–605, Hilton Head Island, SC, USA, June 2000.

[47] G. Tang, L. Zhao, R. Jiang, and X. Zhang, "Single Image Dehazing via Lightweight Multi-scale Networks," in *2019 IEEE International Conference on Big Data (Big Data), Los Angeles*, pp. 5062–5069, Honolulu, HI, USA, 2017.

[48] B. Cai, X. Xu, K. Jia, C. Qing, and D. Tao, "Dehazenet: an end-to-end system for single image haze removal," *IEEE Transactions on Image Processing*, vol. 25, no. 11, pp. 5187–5198, 2016.

[49] K. Tang, J. Yang, and J. Wang, "Investigating haze-relevant features in a learning framework for image dehazing," in *2014 IEEE Conference on Computer Vision and Pattern Recognition*, pp. 2995–3002, Columbus, OH, USA, June 2014.

[50] C. O. Ancuti and C. Ancuti, "Single image dehazing by multi-scale fusion," *IEEE Transactions on Image Processing*, vol. 22, no. 8, pp. 3271–3282, 2013.

[51] B. Li, X. Peng, Z. Wang, J. Xu, and D. Feng, "An all-in-one network for dehazing and beyond," *arXiv: Computer Vision and Pattern Recognition*, 2017.

[52] A. Eitel, J. T. Springenberg, L. Spinello, M. Riedmiller, and W. Burgard, "Multimodal deep learning for robust RGB-D object recognition," in *2015 IEEE/RSJ International Conference on Intelligent Robots and Systems (IROS)*, pp. 681–687, Hamburg, Germany, September 2015.

[53] E. Barshan and P. Fieguth, "Stage-wise training: an improved feature learning strategy for deep models," in *Proceedings of the 1st International Workshop on Feature Extraction: Modern Questions and Challenges*, pp. 49–59, Montreal, Canada, 2015.

[54] S. Ren, K. He, R. Girshick, and J. Sun, "Faster r-cnn: towards real-time object detection with region proposal networks," *IEEE Transactions on Pattern Analysis and Machine Intelligence*, vol. 39, no. 6, pp. 1137–1149, 2017.